Transport integrals and their application to magneto-microwave transmission in n-type germanium and silicon*

A. K. Jain† and G. P. Srivastava
Department of Physics and Astrophysics, Delhi University, Delhi-7, India
(Received 24 August 1973)

This paper presents high-frequency transport integrals involved in the magnetoconductivity tensor of the conduction bands of germanium and silicon. The transport integrals have been defined and studied for a mixture of scatterings due to acoustical phonons, optical phonons, and ionized impurities which have appreciable contribution to the conduction phenomenon in Ge and Si at room temperature. The applications of these integrals to the magneto-microwave properties in Ge and Si are presented and a more accurate analysis of the experimental results on Faraday rotation and magneto-Kerr effect of other workers is attempted. Finally, experimental results on magneto-transmission are presented and analyzed with the help of these integrals in order to determine the relative abundance of impurity scattering and optical-phonon scattering to the acoustic phonon scattering.

I. INTRODUCTION

Microwave techniques[1] are now extensively used to study the transport properties of semiconductors. The transport parameters of semiconductors at high frequency differ from the dc parameters and become complex. Magneto-microwave properties such as magnetoabsorption,[2,3] Faraday rotation,[4–6] and the magneto-microwave Kerr effect[7,8] are the manifestations of the conductivity and the Hall effect at high frequencies. These effects have been studied qualitatively for some fifteen years and used often to estimate the parameters such as effective mass, relaxation time, dielectric constant, or concentration of the charge carriers. Lately, the magneto-microwave Kerr effect and the microwave reflectivity have also been used to study the change in effective mass of the charge carriers with temperature in germanium and silicon.[8]

In the present paper, we investigate various low-field magneto-microwave effects in magneto-transmission in particular, to estimate the relative abundance of various types of scattering mechanisms that influence the conduction phenomena in germanium and silicon at room temperature. The important scattering mechanisms considered in this paper are due to (i) acoustic phonons, (ii) optical phonons, and (iii) the impurities. Other scattering processes such as the carrier-carrier scattering and the neutral-impurity scattering are assumed to be of negligible importance in this temperature range and are not taken into account (see Refs. 9 and 10). The three scatterings mentioned above have been accounted for in the magneto-microwave conductivity through the energy dependence of the relaxation time. These scattering processes are very important to analyze any experimental data at room temperature in semiconductors such as germanium and silicon. The relaxation time accounting for all these three scatterings becomes a complicated function of energy, and the transport integrals cannot be analytically solved. For a combination of impurity scattering and lattice scattering ($\epsilon^{1/2}$), the transport integrals have been numerically solved and tabulated by Dingle *et al.*[11] and Beer *et al.*[12] But no evaluation of the transport integrals for a combination of scatterings due to impurities, acoustic phonons, and optical phonons has been done so far. We have therefore defined the transport integrals for a combination of these three scatterings and generalized them to the high-frequency case in the presence of magnetic fields. These generalized integrals, applicable to the conduction bands of germanium and silicon, have been numerically evaluated for a wide range of scattering parameters which are presented elsewhere.[13] The propogation constants at microwave frequencies of semiconductors placed in the Faraday configuration of magnetic field have been then expressed in terms of these transport integrals and a more accurate analysis of the results on magneto-microwave effects (i.e., Faraday rotation observed by Brodwin and Burgess[6] and Kerr rotation observed by Srivastava and Mehra[14]) has been done. Finally, experimental results on magneto-transmission in n-type silicon and germanium are presented and analyzed by curve-fitting procedures to obtain the scattering parameters denoting the relative abundance of ionized-impurity scattering and optical-phonon scattering to the acoustic-phonon scattering. The values of parameters so obtained have been discussed.

II. MAGNETO-MICROWAVE CONDUCTIVITY AND TRANSPORT INTEGRALS

The microwave conductivity tensor can be derived from the high-frequency generalization of the Boltzmann equation. The components of the conductivity tensor for a cubic semiconductor placed

in a magnetic field, applied in the direction of propagation of microwaves with angular frequency ω, can be written[15]

$$\sigma_{xx} = \sigma_{yy} = \frac{Ne^2}{m^*} \left\langle \frac{\tau(1+j\omega\tau)}{(1+j\omega\tau)^2+\omega_c^2\tau^2} \right\rangle , \quad (1)$$

$$\sigma_{xy} = -\sigma_{yx} = \frac{Ne^2\omega_c}{m^*} \left\langle \frac{\tau^2}{(1+j\omega\tau)^2+\omega_c^2\tau^2} \right\rangle , \quad (2)$$

and

$$\sigma_{zz} = \frac{Ne^2}{m^*} \left\langle \frac{\tau}{1+j\omega\tau} \right\rangle , \quad (3)$$

where e is the electronic charge, m^* is the effective mass, N is the carrier concentration, and τ is the relaxation time of the charge carriers. ω_c is the cyclotron-resonance frequency given by $\omega_c = eB/m^*$ and the angular brackets $\langle\ \rangle$ denote the energy average over the charge carriers of the Maxwellian type defined by

$$\langle F(x)\rangle = \int_0^\infty F(x)e^{-x}x^{3/2}dx \Big/ \int_0^\infty e^{-x}x^{3/2}dx . \quad (4)$$

It is customary and convenient to analyze the propagation of electromagnetic waves in the Faraday configuration in terms of the circularly polarized electric fields rotating in the plane perpendicular to the magnetic field.

The propagation constants for the two senses of polarization characterized by the signs + and − , are determined by the conductivity terms

$$\sigma_\pm \equiv \sigma_{xx} \pm j\sigma_{xy} = \frac{Ne^2}{m^*} \left\langle \frac{\tau}{1+j(\omega\pm\omega_c)\tau} \right\rangle . \quad (5)$$

On separating the real and imaginary parts of (5) we get

$$\sigma_\pm^R = \frac{Ne^2}{m^*} \left\langle \frac{\tau}{1+\nu_\pm^2\tau^2} \right\rangle \quad (6)$$

and

$$\sigma_\pm^I = \frac{Ne^2}{m^*} \nu_\pm \left\langle \frac{\tau^2}{1+\nu_\pm^2\tau^2} \right\rangle , \quad (7)$$

where

$$\nu_\pm = \omega \pm \omega_c .$$

$\sigma_\pm^R$ and $\sigma_\pm^I$ signify the most important feature of the high-frequency conduction and denote the contributions to the in-phase (conductivity) and the out-of-phase (dielectric constant) components, respectively, of the propagating radiation. Investigation of magneto-microwave properties basically involves evaluation of these terms.

Germanium and silicon are characterized by sets of prolate ellipsoidal constant-energy surfaces arranged in reciprocal space to preserve the cubic symmetry. The effective mass and the relaxation time, thus, are highly anisotropic. Herring and Vogt[9] obtained the expression for dc conductivity and Hall effect applied to such a system in terms of the tensor elements $\tau_\perp$ and $\tau_\parallel$ of the anisotropic relaxation time, and $m_\perp$ and $m_\parallel$ of the anisotropic effective mass, which Champlin[16] generalized to the high-frequency case. Since the conductivity and low-field Hall effect are isotropic for cubic semiconductors, it is convenient to write the expression for the effective mass and the relaxation time in analogy with those for the isotropic model, thus giving rise to the concept of conductivity and Hall effective masses m_c and m_H, and relaxation times, τ_c and τ_H, respectively, as given by Champlin and Hauge.[8] Inspection of the conductivity terms $\sigma_\pm^R$ and $\sigma_\pm^I$ for the circularly polarized electric field [Eqs. (6) and (7)] reveals that the well-known results of conductivity and Hall effect for arbitrary high magnetic field can be obtained by substitution of the angular frequency $\omega = 0$ in Eqs. (6) and (7). In other words, $\sigma_\pm^R$ and $\sigma_\pm^I$ can be thought of as the high-frequency modifications of the conductivity and the Hall-effect terms, respectively. Therefore the effective mass and the relaxation time occurring in expressions for $\sigma_\pm^R$ and $\sigma_\pm^I$ could be conveniently replaced by m_c and τ_c in $\sigma_\pm^R$ and m_H and τ_H in $\sigma_\pm^I$. The high-frequency conductivity terms then, can be conveniently written

$$\sigma_\pm^R = \frac{Ne^2}{m_c} \left\langle \frac{\tau_c}{1+\nu_\pm^2\tau_c^2} \right\rangle , \quad (8)$$

$$\sigma_\pm^I = \frac{Ne^2}{m_H} \nu_\pm \left\langle \frac{\tau_H^2}{1+\nu_\pm^2\tau_H^2} \right\rangle , \quad (9)$$

$$\sigma_{zz} = \frac{Ne^2}{m_c} \langle \tau_c \rangle . \quad (10)$$

The effective mass used in $\nu_\pm$ in the above expressions is the cyclotron effective mass as defined by Dresselhaus *et al.*[17]

The energy averages of the type used in the equations above are usually expressed in terms of transport integrals. For isotropic scattering by a single process[15] or a mixture of two processes, these integrals have been defined and tabulated for a wide range of parameters.[11] But for the case of scattering due to a mixture of three processes, general evaluation of the transport integrals has not yet been done. The need of these integrals arises in analyzing the data at room temperature where all the three types of scattering become equally important, e.g., in moderately doped germanium and silicon. We have evaluated the energy averages of the type used in Eqs. (9)–(11) for the conduction bands of germanium and silicon for a wide range of scattering coefficients.[13] The integrals can be applied to the conduction phenomena in samples of a wide range of conductivity at magnetic fields in the range such that $(\omega \pm \omega_c)\tau_0 = \pm 10$. The transport integrals have been defined as a

function of the product $\nu\tau_0$, where τ_0 is the energy-independent relaxation time. The energy dependence of relaxation time and the anisotropy of the scattering is accounted for in the factor $F_{\perp,\parallel}$ defined

$$\tau_{\perp,\parallel} = \tau_0 F_{\perp,\parallel} . \tag{11}$$

The energy dependence of $F_{\perp,\parallel}$ is given by

$$F_{\perp,\parallel}(x, T) = C^a_{\perp,\parallel}(T/\Theta)^{3/2}x^{1/2} + C^i_{\perp,\parallel} W_I (T/\Theta)^{-3/2}x^{-3/2} + W_0\{e^{\Theta/T}-1\}^{-1}\{(xT/\Theta+1)^{1/2} + e^{\Theta/T}(xT/\Theta-1)^{1/2}\delta(x-\Theta/T)\} , \tag{11a}$$

where the first term in the above expression accounts for the scattering due to acoustic phonons or lattice,[9] the second term is for the ionized-impurity scattering,[18] and the third term denotes the scattering due to the optical phonons.[19] The anisotropy of the lattice and the impurity scattering is accounted for through the factors $C^a_{\perp,\parallel}$ and $C^i_{\perp,\parallel}$, respectively. The optical-phonon scattering due to intervally absorption or emission of phonons is considered to be isotropic since the valleys in germanium and silicon are quite far apart, so that all the intervalley transitions are in the same direction. Intervalley optical-mode scattering is of the same type in nature as the intervalley optical-mode scattering and can be taken into account by the same term. The relative abundance of the impurity and optical-phonon scattering to the acoustic-phonon scattering is given by the coefficients W_I and W_0, respectively, and Θ is the Debye temperature.

The conductivity and the Hall-effect relaxation times can now be written in terms of $F_\perp$ and $F_\parallel$ as

$$\tau_c \equiv \tau_0 F_c = \tau_0\left(\frac{2K_m F_\perp + F_\parallel}{2K_m + 1}\right) \tag{12}$$

and

$$\tau_H \equiv \tau_0 F_H = \tau_0\left(\frac{K_m F_\perp^2 + 2F_\perp F_\parallel}{K_m + 2}\right)^{1/2} . \tag{13}$$

With the help of Eqs. (8)–(10), we can now define the transport integrals as

$$I_c = \frac{1}{\Gamma_{(5/2)}}\int_0^\infty \frac{\gamma F_c}{1+\gamma^2 F_c^2} x^{3/2}e^{-x}dx , \tag{14}$$

$$I_H = \frac{1}{\Gamma_{(5/2)}}\int_0^\infty \frac{\gamma^2 F_H^2}{1+\gamma^2 F_H^2} x^{3/2}e^{-x}dx , \tag{15}$$

and

$$I_0 = \frac{1}{\Gamma_{(5/2)}}\int_0^\infty F_c x^{3/2}e^{-x}dx ; \tag{16}$$

$$\gamma = \nu\tau_0 ,$$

such that the conductivity terms can be written down in terms of I_c, I_H, and I_0 as following:

$$\sigma^R_\pm = \frac{Ne^2}{m_c\nu_\pm} I_c , \tag{17}$$

$$\sigma^I_\pm = \frac{Ne^2}{m_H\nu_\pm} I_H , \tag{18}$$

$$\sigma \equiv \sigma_{zz} = \frac{Ne^2}{m_c}\tau_0 I_0 . \tag{19}$$

The numerical evaluation and the tabulation of these integrals for W_0 and W_I varying from 0.001 to 10.0 for the conduction bands of germanium and silicon at room temperature are presented elsewhere.[13] For n-type germanium these integrals are graphically illustrated in Fig. 1. The importance of various scattering coefficients is quite evident from these curves. Expressions (17)–(19) will be used in Sec. III to analyze the magneto-microwave effects.

III. MAGNETO-MICROWAVE EFFECTS IN THE FARADAY CONFIGURATION

The propagation constants corresponding to the two senses of polarization of the propagating electromagnetic wave through an axially magnetized semiconducting medium are given by

$$\mu_\pm \equiv (\alpha_\pm - j\beta_\pm)^2 = \omega^2\mu_0\epsilon_\pm , \tag{20}$$

where μ_0 is the permeability of free space and $\epsilon_\pm$ is the effective dielectric constant of the media given by

$$\epsilon_\pm \equiv (\epsilon^R_\pm + j\epsilon^I_\pm) = \epsilon_{st} - \sigma^I_\pm/\omega + j\sigma^R_\pm/\omega , \tag{21}$$

where ϵ_{st} is the dielectric constant of the carrier-free medium. Using Eqs. (17)–(19), we can write down the expression for the refractive indices $n_\pm$ and the absorption constant $k_\pm$

$$n_\pm = \frac{1}{\sqrt{2}}\left\{\left(\epsilon_{st} - \xi\frac{I_H}{m_H}\right) + \left[\left(\epsilon_{st} - \xi\frac{I_H}{m_H}\right)^2 + \left(\xi\frac{I_c}{m_c}\right)^2\right]^{1/2}\right\} \tag{22}$$

and

$$k_\pm = \frac{1}{\sqrt{2}}\left\{-\left(\epsilon_{st} - \xi\frac{I_H}{m_H}\right) + \left[\left(\epsilon_{st} - \xi\frac{I_H}{m_H}\right)^2 + \left(\xi\frac{I_c}{m_c}\right)^2\right]^{1/2}\right\} , \tag{23}$$

where

$$\xi = Ne^2/\omega\nu_\pm .$$

To account for the guided-wave correction

$(\epsilon_{st} - \xi I_H/m_H)$ is simply multiplied by a factor $1-(\omega_{co}/\omega)^2$, where ω_{co} is the cutoff frequency of the wave guide. Knowing $n_\pm$ and $k_\pm$ one can directly get the expressions for $\alpha_\pm$ and $\beta_\pm$ also, using Eq. (20).

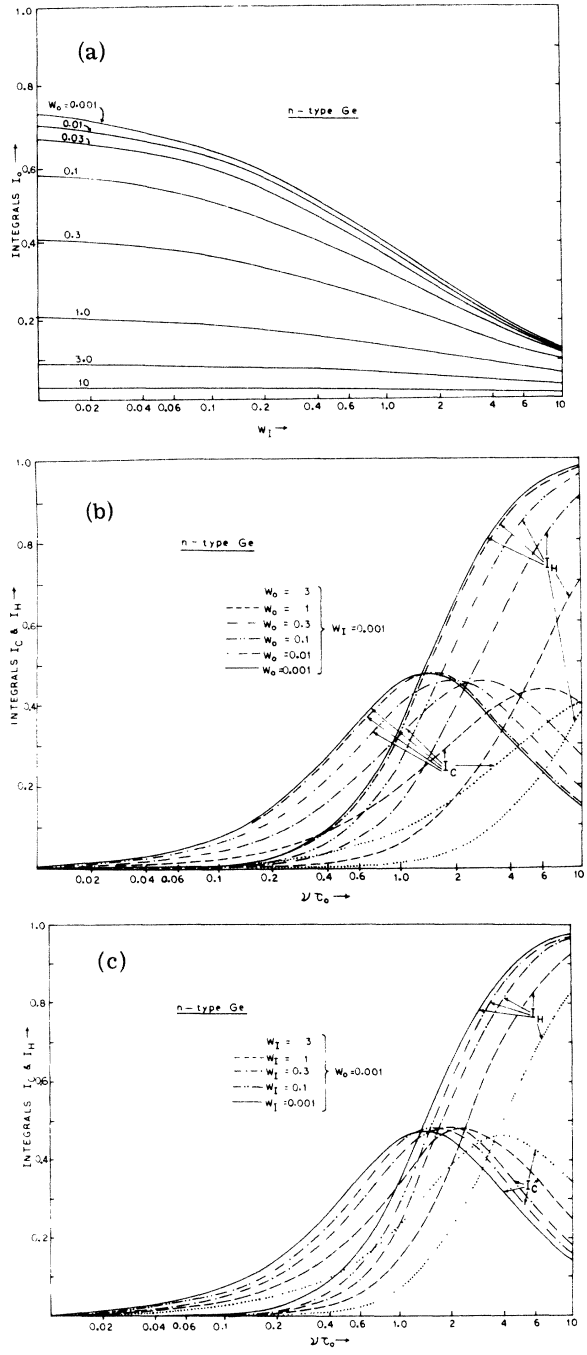

FIG. 1. (a) Integrals I_0 for the conduction band of germanium at room temperature. (b) Integrals I_c and I_H as functions of $\nu\tau_0$ for various values of W_0 and $W_I = 0.001$. (c) Integrals I_c and I_H as functions of $\nu\tau_0$ for various values of W_I and $W_0 = 0.001$.

Once the complex dielectric constant or the complex propagation constant is known, the magneto-microwave effects can be worked out using standard formulations. The power transmission and reflection from a sample of finite thickness and the detailed theory of Faraday rotation in semiconductors of finite thickness has been worked out by Donovan and Medcalf[20] and Bouwknegt and Volger.[21] We have used the expressions of Donovan and Medcalf for the analysis. The magneto-Kerr effect at microwave frequencies has been analyzed by Brodwin and Vernon[7] in terms of the orthogonal components of the reflected ellipse; for an axially magnetized semiconductor, the ratio of these amplitudes R_g, and the phase difference ϕ, between them. The detailed expressions for these effects will be a repetition of the work of other authors referred to above, and are not presented in this paper.

The power transmission and reflection for circularly polarized modes as well as linear polarization, the Faraday rotation θ, and the ratio of the orthogonal components R_g (Kerr effect) have been numerically computed for a test sample of n-type germanium of resistivity 15 Ωcm, for various scattering coefficients W_0 and W_I, to study their effect on the physical quantities. The coefficient W_I characterizes the impurity scattering in the material and hence the number of carriers the material is doped with, while the coefficient W_0 indicates the optical-phonon scattering and depends on the growth of the crystals. These coefficients have been normalized with the acoustical-phonon scattering coefficient, which, therefore, it taken to be unity in expression (11a). The influence of W_0 and W_I on the physical quantities such as transmission, reflection, Faraday rotation, and ratio of the orthogonal components of reflected wave is clearly illustrated in Figs. 2–4.

Figure 2 shows power transmission $T_\pm$ and reflection $R_\pm$ for the circularly polarized modes. Figure 3 illustrates the Faraday rotation θ and in Fig. 4 R_g is drawn as a function of dc magnetic field applied in the direction of propagation. The two modes of circular polarizations are plotted against the opposite signs of the magnetic field in Fig. 2. Invariably, all the quantities show inversions at higher values of magnetic field which is the indication of the commencement of the magnetoplasma edge.[22]

It is evident from the figures that the two scattering coefficients have the opposite influence on the magnitude of $T_\pm$, $R_\pm$, θ, and R_g. At lower fields below the plasma edge, an increase in W_I decreases the magnitude—although not so influentially as W_0. This is quite expected at room temperature. The scattering coefficients have much more significant effects at high magnetic fields, i.e., beyond the maxima where even the roles of W_0 and

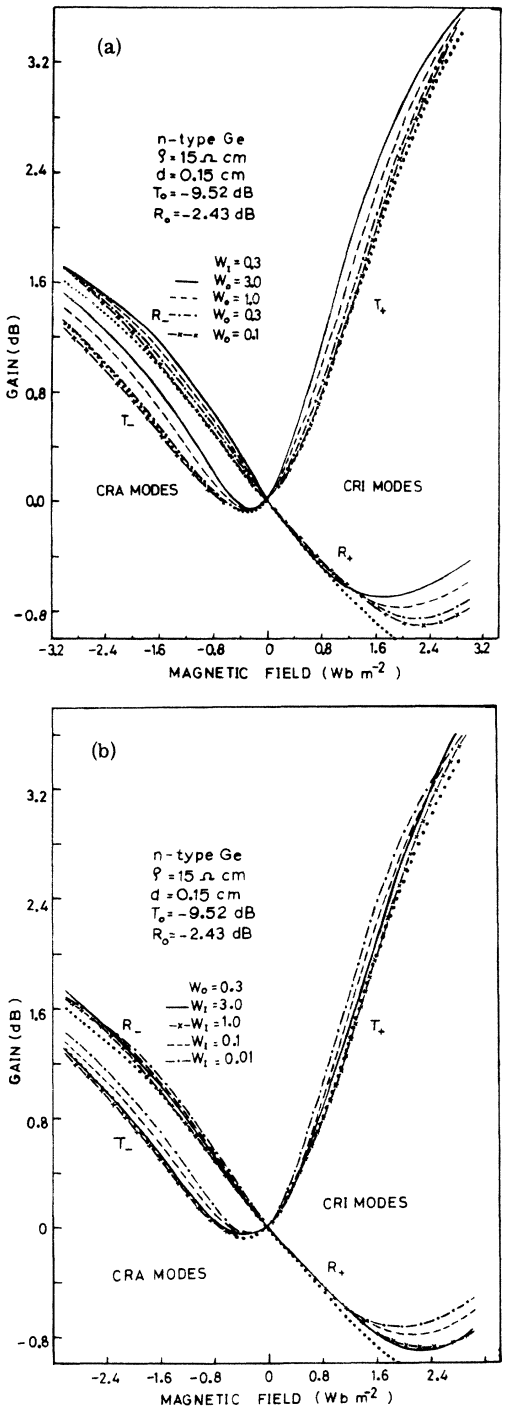

FIG. 2. (a) Effect of the scattering parameter W_0 on transmission and reflection on an n-type germanium sample at room temperature. The dotted curves are plotted for the energy-independent relaxation time. (b) Effect of the scattering parameter W_I on transmission and reflection on an n-type germanium sample at room temperature. The dotted curves are plotted for the energy-independent relaxation time.

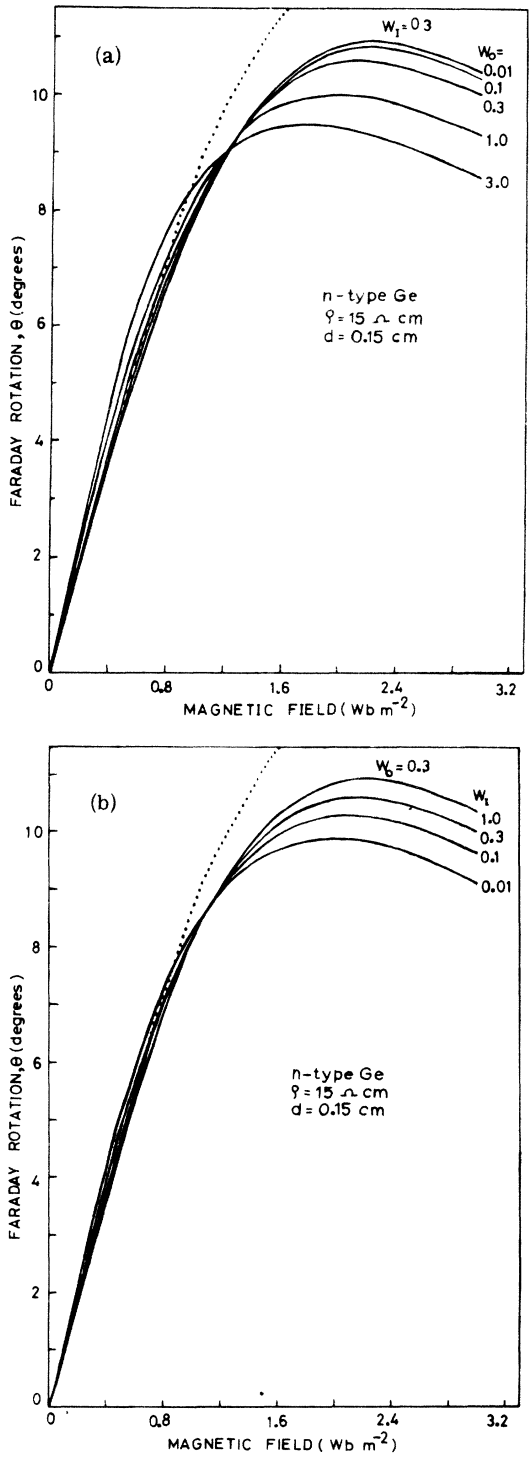

FIG. 3. (a) Effect of the scattering parameters W_0 on Faraday rotation on an n-type germanium sample at room temperature. The dotted curves are plotted for the energy-independent relaxation time. (b) Effect of the scattering parameter W_I on Faraday rotation on an n-type germanium sample at room temperature. The dotted curves are plotted for the energy independent relaxation time.

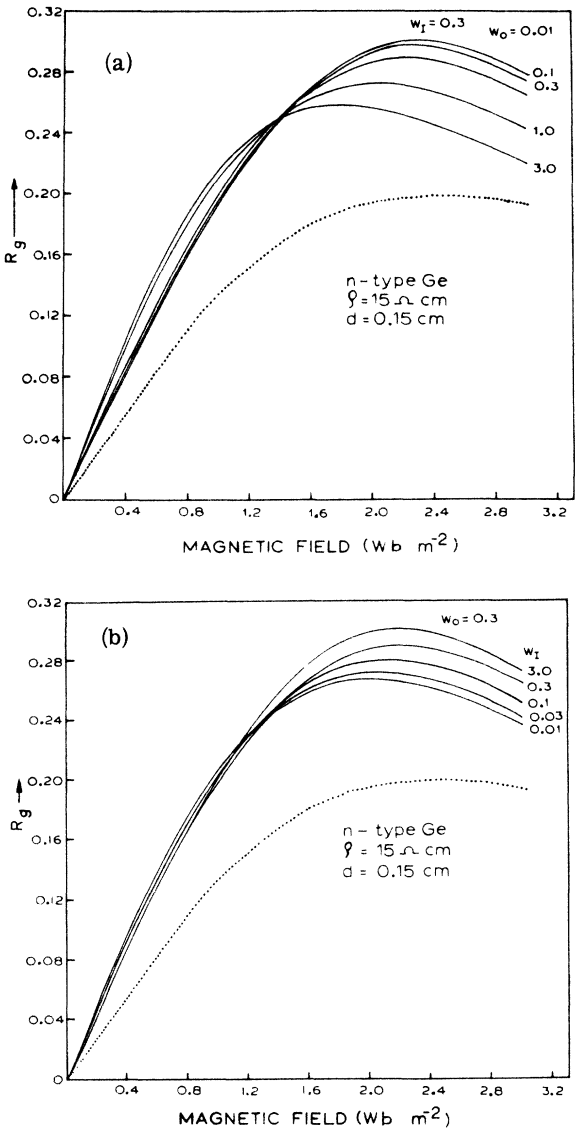

FIG. 4. (a) Effect of the scattering parameter W_0 on the Kerr effect on an n-type germanium sample at room temperature. The dotted curves are plotted for energy-independent relaxation time. (b) Effect of the scattering parameter W_I on the Kerr effect on an n-type germanium sample at room temperature. The dotted curves are plotted for energy-independent relaxation time.

W_I to affect the magnitudes of $T_\pm, R_\pm$, θ, and R_g, are reversed. It is interesting to note that W_0 has a significant influence on the position of maxima. With an increase in W_0, the maximum shifts towards the lower magnetic fields. This provides a satisfactory explanation to the results of Furdyna and Broersma[23] who observed the maxima in Faraday rotation to vary between $\omega_c \tau = 1.0$–1.4.

Brodwin and Burgess[24] have observed Faraday rotation in Ge and Si at room temperature up to 15.0 Wb/m^2 with the use of pulsed magnetic fields and compared these results with the theoretical calculations based on ellipsoidal lattice-scattering model. Although the agreement has been shown to be fairly good at low fields, there is significant departure of the experimental results from theoretical calculations at higher fields. No probable explanation was given to this anomaly. It is felt that this anomaly is due to the fact that impurity scattering was not taken into account. We have tried to explain their results on the basis of the scattering model discussed in Sec. II. Computer calculations are done for one of their samples—n-type germanium. Using their conductivity data, the scattering coefficients W_0 and W_I have been adjusted to obtain a better fit with their experimental data. Figure 5(a) presents a comparison of the theoretical curves computed by them and the authors, to fit the experimental results. The values of W_0 and W_I used for the best fit are indicated.

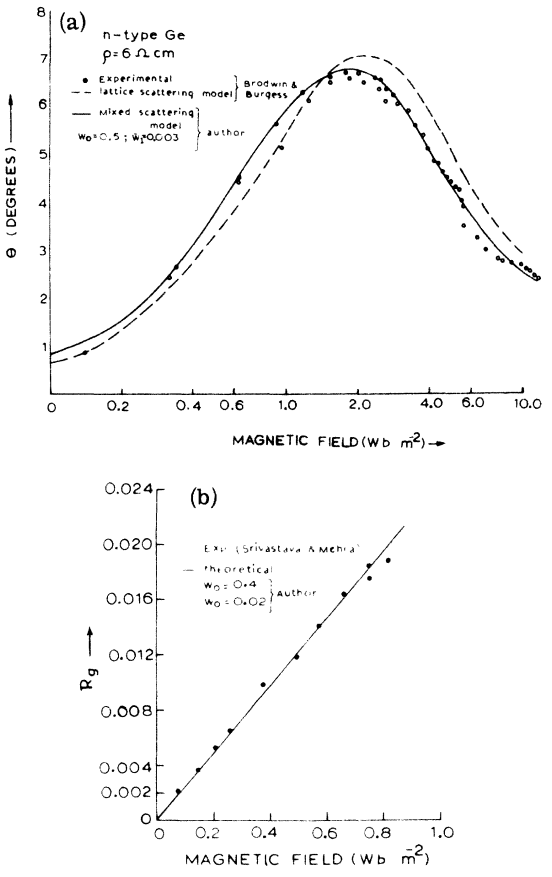

FIG. 5. (a) Comparison of experimental results of Brodwin and Burgess (Ref. 24) on Faraday rotation in germanium with their theoretical curve and the authors'. (b) Comparison of experimental results of Srivastava and Mehra (Ref. 14) on the Kerr effect with the theoretical curve of the authors.

TABLE I. Scattering parameters for silicon samples over the temperature range 150–273 °K.

Sample number	Sample	Orientation[a]	Carrier concentration (m^{-3})	Conductivity ($\Omega^{-1}\,m^{-1}$)	W_0	W_I
1	SiN-I	⟨111⟩	1.02×10^{21}	21.0	1.5	0.06
2	SiN-II	⟨111⟩	4.8×10^{20}	10.0	1.5	0.016
3	Si (Champlin and Hauge)[b]		•••	•••	2.0	0.15

[a]Crystallographic axis with respect to magnetic field. [b]Reference 8.

An excellent agreement between the experimental results on R_g in an n-type-germanium sample obtained by Srivastava and Mehra,[14] and the theoretical calculations by the authors is presented in Fig. 5(b). Unfortunately, no experimental data of R_g beyond 0.8 Wb/m^2 could be found in the literature to prove the applicability of the present model.

IV. ANALYSIS OF EXPERIMENTAL DATA ON TRANSMISSION

Straight-through transmission in two n-type-silicon and two n-type-germanium samples (see Table I) has been studied as a function of magnetic field at room temperature (293 °K) and 150 °K. The experimental setup used for the measurements was essentially the same as described by the authors in one of their earlier papers.[25] The magnetic field was applied in the direction of propagation using an electromagnet with an axial hole in its pole pieces through which the circular waveguide containing the sample passes such that the sample was placed in the center of the field. The sample in the form of a circular disc was mounted in the waveguide so as to cover its cross section completely. The power leakage through the small gap between the sample and the waveguide walls was found to be negligible and was further minimized by using silver conducting paint at the joints. The transmission for both senses of circular polarization was studied up to 0.7 Wb/m^2. The sense of polarization was changed by simply reversing the direction of the magnetic field. To observe the small changes in the transmission due to the magnetic field, the transmitted signal after detection was compared with the reference signal obtained from the directional coupler before the sample, in the difference amplifier.

A. n-silicon

The experimental data on the two n-type silicon samples at 293 and 152 °K are presented in Figs. 6(a) and 6(b), respectively. The gain in transmitted power for both the modes of polarization is plotted against the magnetic field—the, cyclotron-resonance-active[22] (CRA) mode against the negative values and the clyclotron-resonance-inactive[22] (CRI) mode against the positive values of magnetic fields. For the analysis, the static dielectric constant was taken to be 11.6 and the values of effective masses used were $m_{\parallel}=0.98m_e$ and $m_{\perp}=0.19m_e$,

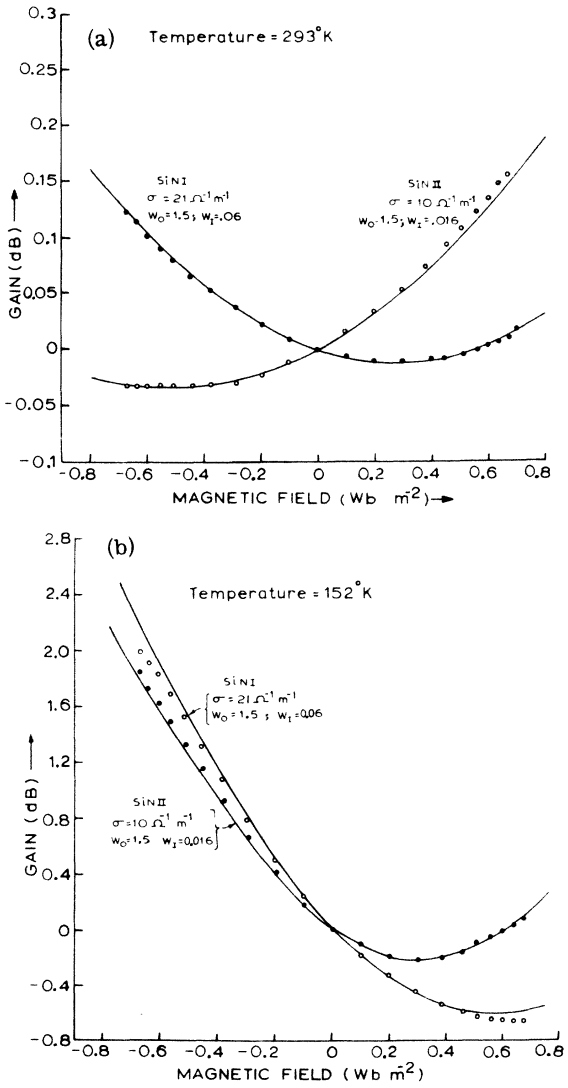

FIG. 6. (a) Grain in transmitted power as a function of magnetic field at 293 °K for the two silicon samples, SiN-I and SiN-II. (b) Gain in transmitted power as a function of magnetic field at 152 °K for the two silicon samples, SiN-I and SiN-II.

respectively.[26] Following Ham the values of $C_{\parallel}^{a}/C_{\perp}^{a}$ and $C_{\parallel}^{i}/C_{\perp}^{i}$ were taken to be 1.5 and 0.25.[27] A large component of optical-mode intervalley scattering is obvious from the temperature dependence ($T^{-2.6}$) of the mobility, whereas the intravalley optical-phonon scattering in silicon had been pointed out to be negligible in this temperature range by Harrison.[28] An analysis of all the possible intervalley transitions in silicon from neutron scattering measurements by Long[29] suggested the characteristic temperature to be 630 °K.

To determine the scattering parameters W_0 and W_I for the sample, preliminary estimations were made from the temperature dependence of conductivity which was calculated for a number of sets of W_0 and W_I for each sample and compared with the experimentally obtained curves. The parameters W_0 and W_I were then used to calculate the magnetic field dependence of transmitted power using the integrals I_c, I_H, and I_0 defined in Eqs. (14)–(16). Slight variations were then made in W_0 and W_I to fit the calculated curves for gain in transmitted power with the experimental data. W_0 was varied to improve the curve fitting at room temperature while W_I was used to improve the fit at low temperature. The values of W_0 and W_I obtained were then used again to compare the conductivity curves as a final check (Fig. 7). A comparison of experimental curves and the theoretical curves obtained using the estimated scattering parameters is presented in Figs. 6(a) and 6(b) for the two silicon samples. For comparison's sake, the values of scattering parameters obtained by Champlin and Hauge[8] for one silicon sample are presented in Table II along with our results. The optical-phonon scattering parameter W_0 as obtained for our samples differed slightly from Hauge's sample, which we attribute to the growth of the samples. Though no direct reason can be given for the low values of W_I obtained for our samples, it must be mentioned that the parameters obtained by Champlin and Hauge[8] were obtained from dc measurements while we have throughout used the microwave data in our analysis.

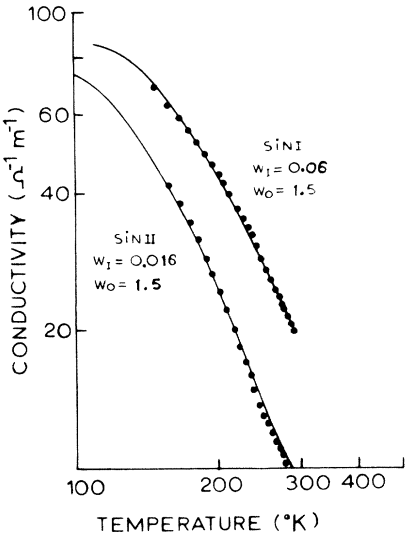

FIG. 7. Experimental points and theoretical curves of conductivity for the two silicon samples. The values of the scattering parameters obtained are indicated against the curves.

B. *n*-germanium

The results on gain in transmitted power in germanium at 293 and 150 °K are presented in Figs. 8(a) and 8(b). The conductivity variation with temperature for these two samples shows intrinsic behavior near room temperature. This indicates that both types of carriers contribute appreciably to the transport phenomenon and must be accounted for. For such samples the carrier concentration cannot be assumed to be constant. The number of electrons and holes present at any temperature are estimated by studying the temperature variation of the transmitted power in the temperature range in which the change from extrinsic to the intrinsic behavior takes place. (The details of the method are discussed in the thesis of Jain.[13])

To account for both types of carriers in these samples, Eqs. (8) and (9) were modified to

TABLE II. Scattering parameters for germanium samples over the temperature range 150–273 °K.

Sample number	Sample	Orientation[a]	Excess of electrons (m^{-3})	Conductivity (Ω^{-1} m^{-1})	W_0	W_I
1	Ge441*A*	⟨110⟩	1.5×10^{20}	6.8	0.2	0.006
2	Ge457*A*	⟨110⟩	0.75×10^{20}	4.0	0.2	0.002
3	Ge (Champlin and Hauge)[b]	···	···	2.0	0.2	0.00
4	Ge (Brodwin and Burgess)[c]	···	2.6×10^{20}	10.67	0.5	0.004
5	Ge (Srivastava and Mehra)[d]	···	5.3×10^{20}	33.34	0.4	0.02

[a]Crystallographic axis with respect to magnetic field.
[b]Reference 8.
[c]Reference 24.
[d]Reference 14.

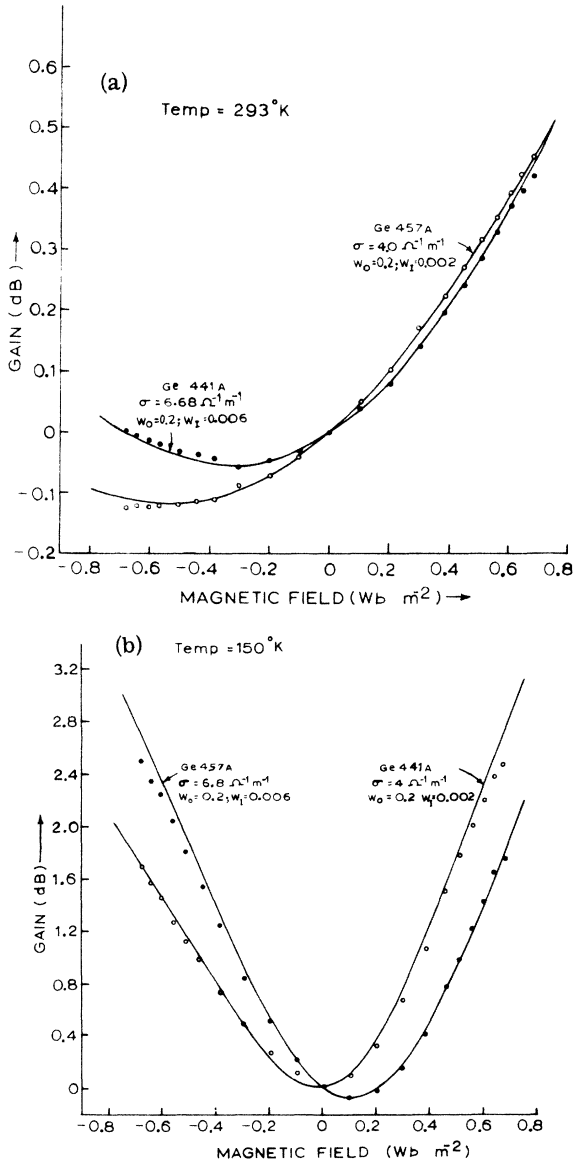

FIG. 8. (a) Gain in transmitted power as a function of magnetic field at 293 °K for the two germanium samples, Ge441*A* and Ge457*A*. (b) Gain in transmitted power as a function of magnetic field at 150 °K for the two germanium samples, Ge441*A* and Ge457*A*.

$$\sigma_{\pm}^{R} = \frac{Ne^2}{m^*}\left\langle \frac{\tau}{1+\nu_{\pm}^2\tau^2}\right\rangle + \frac{Pe^2}{m^{*\prime}}\left\langle \frac{\tau'}{1+\nu_{\pm}'^2\tau'^2}\right\rangle \tag{24}$$

and

$$\sigma_{\pm}^{I} = \frac{Ne^2}{m^*}\left\langle \frac{\tau^2}{1+\nu_{\pm}^2\tau^2}\right\rangle \nu_{\pm} + \frac{Pe^2}{m^{*\prime}}\left\langle \frac{\tau'^2}{1+\nu_{\pm}'^2\tau_{\pm}'^2}\right\rangle \nu_{\pm}', \tag{25}$$

where P is the number of holes per unit volume. The unprimed quantities correspond to electrons, while the primed ones to holes.

Since the samples used here are n type, the contribution of holes to the transmission is very small and becomes negligible at low temperatures. We therefore have done detailed calculations for the electron contribution [first term in Eqs. (24) and (25)] in the same way as for silicon, and the hole contribution is calculated using the established results for intrinisic mobility and $m^{*\prime} = 0.276 m_e$.[15] The scattering parameters W_0 and W_I are then estimated from the transmission curves in the same way as for silicon. A comparison of the experimental curves with the theoretical curves using the determined values of W_0 and W_I is presented in Figs. 8(a), 8(b), and 9. Table II describes the scattering parameters for our samples and the samples of other workers. The otpical-phonon parameter W_0 for our samples compares well with the sample of Champlin and Hauge[8] while for the samples 3 and 4 of Table V, W_0 is higher, which might be due to the growth of the samples. The lattice deformations, etc., affect the optical-phonon scattering. The impurity scattering parameter W_I increases with the conductivity of the samples except for sample 4. This discrepancy might have been due to different experimental techniques, conditions, and measurement of a different phenomenon. The parameters for sample 4 are estimated from the Faraday-rotation measurements of Brodwin and Burgess[24] for pulsed magnetic fields.

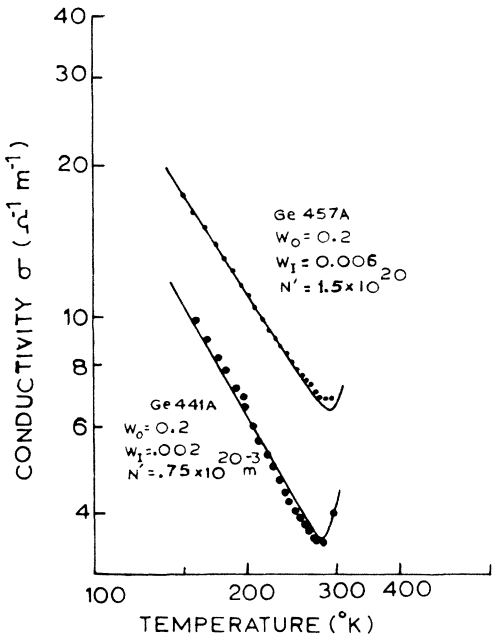

FIG. 9. Experimental points and the theoretical curves of conductivity for the two germanium samples. The values of the scattering parameters are indicated against each curve.

V. CONCLUSION

The analysis of free-carrier magneto-microwave effects in terms of frequency- and magnetic-field-dependent conductivity tensor through the transport integrals, provides a unified treatment of the phenomena. This allows the inclusion of a combination of scattering processes (isotropic or anisotropic) where these scatterings can be expressed in terms of relaxation time. The components of the conductivity tensor are expressed directly in terms of the tabulated transport integrals for combination of scattering processes due to acoustic phonons, optical phonons, and impurities. Further, an accurate study of magneto-microwave properties leads to more information regarding the scattering mechanisms.

The study of these effects up to higher magnetic fields could yield even more useful results. The theory could also be extended to include the cases where relaxation time cannot be defined, as for polar scattering through variational methods.

ACKNOWLEDGMENTS

The authors would like to thank R. M. Mehra for useful discussions. One of the authors (A.K.J.) also acknowledges the Council of Scientific and Industrial Research (India) for the scholarship award during the completion of the project.

---

*Work forms a part of the Ph.D. thesis of A. K. Jain submitted to the University of Delhi.

†Present address: Clarendon Laboratory, Oxford, OX1 3PU, United Kingdom.

[1]D. W. Griffin (private communication).

[2]J. K. Furdyna and M. E. Brodwin, Phys. Rev. 132, 97 (1963).

[3]A. Libchaber and R. Veilex, Phys. Rev. 127, 774 (1962).

[4]R. R. Rau and M. E. Caspari, Phys. Rev. 100, 632 (1955).

[5]B. Donovan and J. Webster, (a) Proc. Phys. Soc. Lond. 79, 46 (1962); (b) Proc. Phys. Soc. Lond. 79, 1087 (1962).

[6]K. S. Champlin, Physica (Utr.) 28, 1143 (1962).

[7]M. E. Brodwin and J. Vernon, Phys. Rev. 140, A1390 (1965).

[8]K. S. Champlin and P. S. Hauge, J. Appl. Phys. 39, 4099 (1968).

[9]C. Herring and E. Vogt, Phys. Rev. 101, 944 (1956).

[10]G. L. Parson, W. T. Read, Jr., and F. J. Morin, Phys. Rev. 93, 666 (1954).

[11]R. B. Dingley, P. Arndt, and S. K. Roy, Appl. Sci. Res. B 6, 755 (1956).

[12]A. C. Beer, J. A. Armstrong, and I. N. Greenberg, Phys. Rev. 107, 1506 (1957).

[13]A. K. Jain, Ph.D. thesis (Delhi University, 1972) (unpublished).

[14]G. P. Srivastava and R. M. Mehra, Indian J. Pure Appl. Phys. 9, 736 (1971).

[15]G. P. Srivastava and A. K. Jain, J. Phys. C 4, 364 (1971).

[16]K. S. Champlin, Phys. Rev. 130, 1374 (1963).

[17]G. Dresselhaus, A. K. Kip, and C. Kittel, Phys. Rev. 100, 618 (1955).

[18]N. Brooks, Phys. Rev. 83, 879 (1951).

[19]C. Herring, Bell System Tech. J. 34, 237 (1955).

[20]B. Donovan and T. Medcalf, Brit. J. Appl. Phys. 15, 1139 (1964).

[21]A. Bouwknegt and J. Volgev, Physica (Utr.) 30, 113 (1964).

[22]J. K. Furdyna, Appl. Optics 6, 675 (1967).

[23]J. K. Furdyna and S. Broersma, Phys. Rev. 120, 1995 (1960).

[24]M. E. Brodwin and T. J. Burgess, Appl. Phys. Lett. 5, 224 (1964).

[25]G. P. Srivastava and A. K. Jain, Rev. Sci. Instr. 42, 1793 (1971).

[26]R. N. Dexter, H. J. Zeiger, and B. Lax, Phys. Rev. 104, 637 (1956).

[27]S. Ham, Phys. Rev. 100, 1251 (1955).

[28]W. A. Harrison, Phys. Rev. 104, 1281 (1956).

[29]D. Long, Phys. Rev. 120, 2024 (1960).